レーザー逆コンプトンX線光源を用いたフェムト秒時間分解X線研究の可能性

Photon Factory, KEK
Shin-ichi Adachi

- **Motivation**
- **Feasibility**
- **Case study**

光源のエネルギーとパルス幅

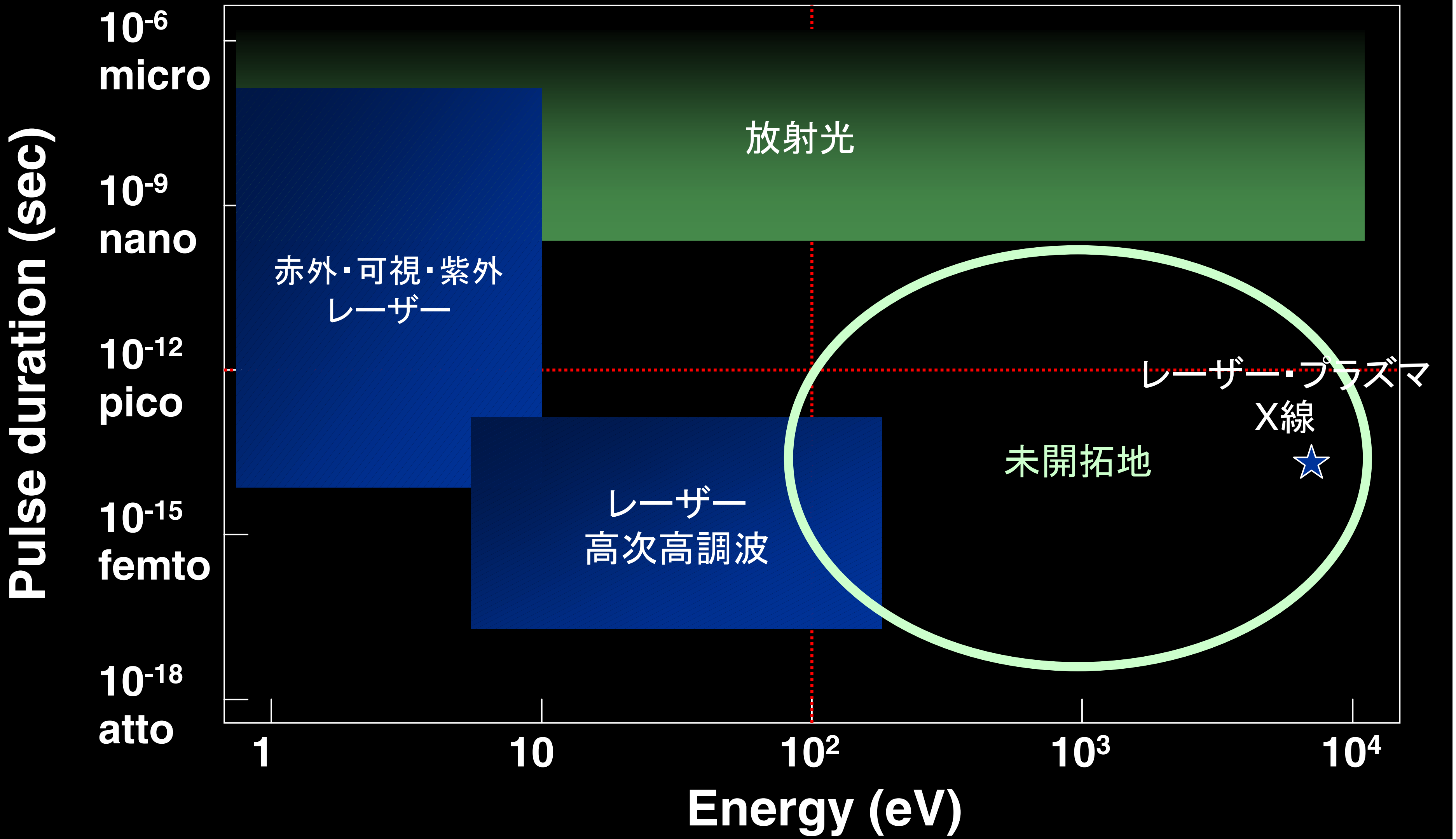

Phonon-polariton wave in $LiTaO_3$ (ALS)

Cavalleri at al. (2006) Nature 442 664.

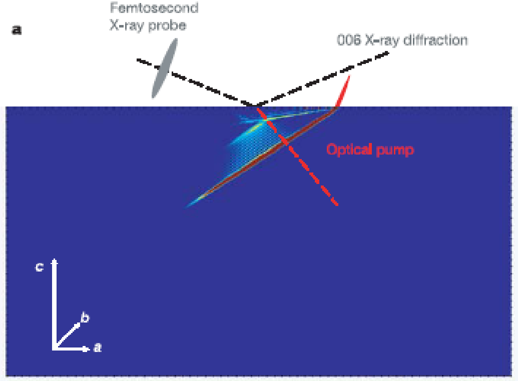

Bond softening in Bismuth (SPPS)

Fritz et al. (2007) Science 315, 633.

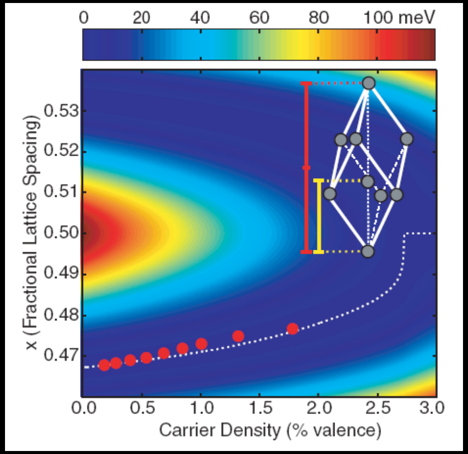

Magnetic excitations in permalloy squares (SLS)

Raabe et al. (2005) Phys. Rev. Lett. 94,217204

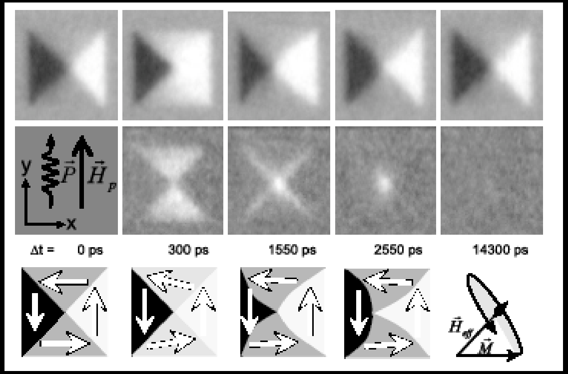

Time Domain Science with SR

最近の報告例

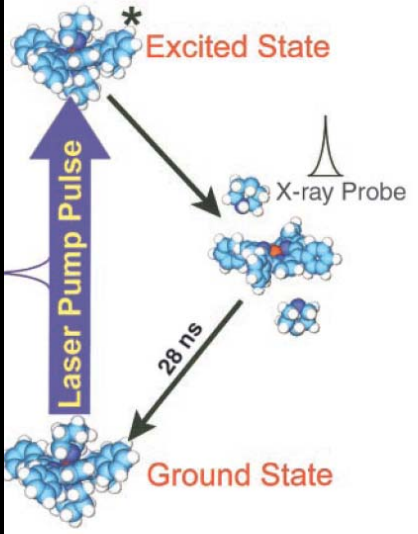

Ni(II) porphyrin (APS)

Chen et al. (2001) Science 292, 262.

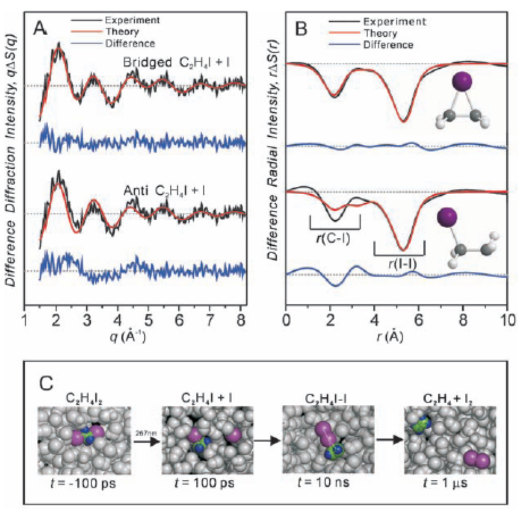

$C_2H_4I_2$ in methanol (ESRF)

Ihee, et al., (2005) Science 309, 1223.

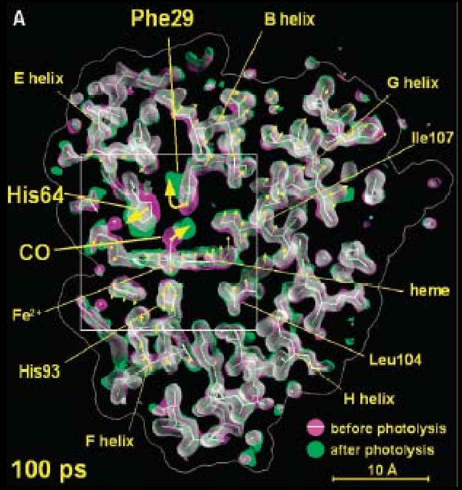

Mutant myoglobin (ESRF)

Schotte et al.(2003) Science 300, 1944.

Femtosecond X-ray Pulses at 0.4 Å Generated by 90° Thomson Scattering: A Tool for Probing the Structural Dynamics of Materials

Schoenlein et al. (1996) **Science** 274, 236.

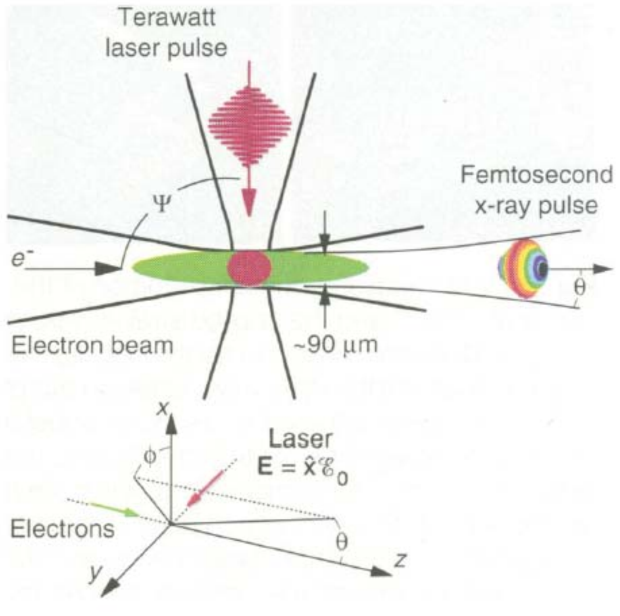

Fig. 1. Schematic of the femtosecond Thomson scattering geometry.

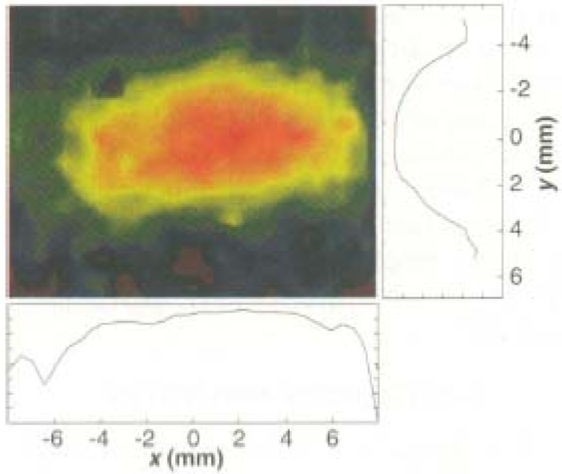

Fig. 2. False-color CCD image of the spatial profile of a 30-keV (0.4 Å), ~300-fs x-ray pulse striking a phosphor screen at a distance of 80 cm from the scattering point. Vertical and horizontal lineouts indicate a beam size of ~12 mm by ~8 mm (FWHM).

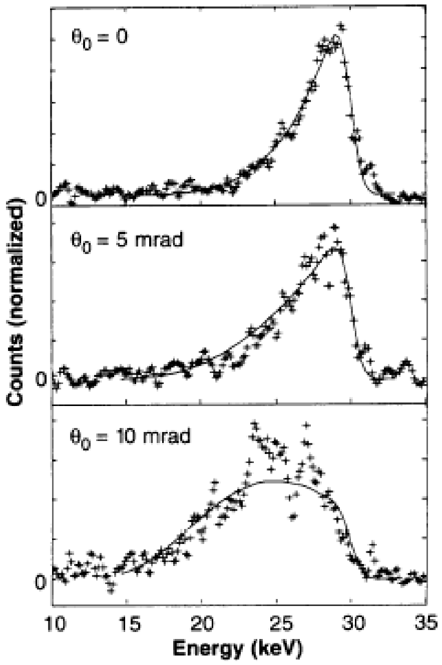

Fig. 3. Spectral measurements of the femtosecond x-rays at observation angles of $\theta_0 = 0$ mrad, 5 mrad, and 10 mrad ($\phi_0 = \pi/2$). The detector lies in the *yz* plane. Also shown (solid lines) are theoretically predicted spectra corrected for detector sensitivity and window transmission as described in the text.

Electron: 50 MeV, 1.3nC, 20 ps (FWHM)
Laser: 60mJ, 100fs, 10Hz, 800 nm
X-ray: 30 keV, ~300fs, 2 x 10^5 photons/pulse/15%

“Rapid advances in diode-pumped, solid state lasers and superconducting linac structures may provide substantially higher x-ray brightness in future Thomson sources by operating at very high repetition rates.”

1996

Electron: 50 MeV, 1.3nC, 20 ps (FWHM)
Laser: 60mJ, 100fs, 10Hz, 800 nm
X-ray: 30 keV, ~300fs, 2×10^5 photons/sec/15%b.w.

2007

Electron: 60 MeV, 1nC, 1 ps
Laser: 1 mJ, 150 fs, 10000 Hz, 800 nm
X-ray: 42 keV, 1×10^{10} photons/sec/10%b.w. !!

Laser-Compton X-ray source at ERL test facility (60-150MeV)

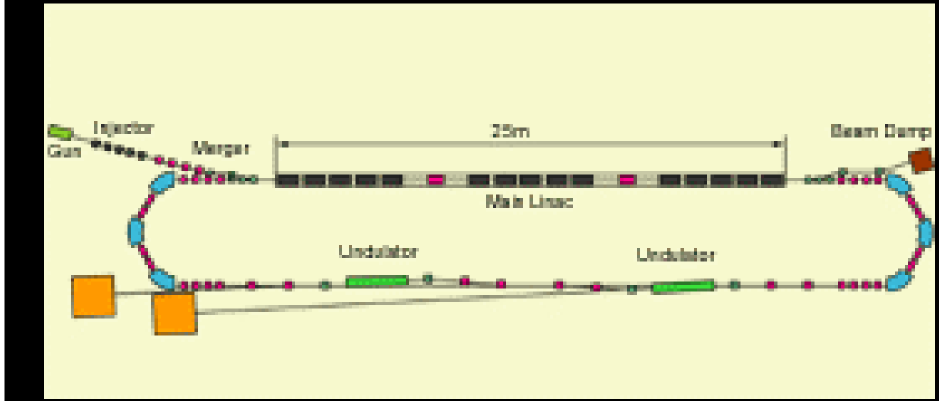

$$E_{Xray} = 2\gamma^2 E_{Laser}(1-\cos\theta_L)/(1+\gamma^2\theta^2)$$

$$Flux = (N_L N_e/wh)(L_{eff}/L_b)\sigma_c$$

$E_{Laser} = 1.55$eV, $E_{electron} = 60$ MeV (γ=117), $\theta_L = 90$ degree のとき、
軸上(θ=0)で**E_{Xray} = 42.4 keV**

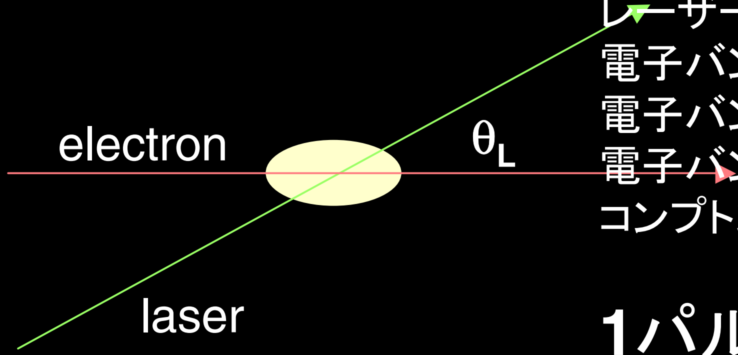

レーザーパルス（1.55eV, 1mJ)のフォトン数：　$N_L = 4 \times 10^{15}$ photons
電子バンチ中の電子数（60MeV, 1nC)：　$N_e = 6 \times 10^9$ electrons
電子バンチの水平幅：　$w = 50 \times 10^{-6}$ m
電子バンチの高さ：　$h = 50 \times 10^{-6}$ m
コンプトン散乱断面積：　1×10^{-28}

1パルスあたり、

Flux = 1×10^6 phs/pulse/10%b.w.

10kHzのとき、

Flux = 1×10^{10} phs/sec/10%b.w.

Source	Pulse length (fs)	Repetition rate (Hz)	Photon flux	Energy range
Compact ERL/Laser-Compton Source (1nC, 10kHz)	~150	10000	1 x 10^{10} phs/sec/10%b.w. 1 x 10^{6} phs/sec/0.1%b.w. 1 x 10^{6} phs/pulse/10%b.w.	10-100 keV
PF-AR NW14 (80nC, 794kHz, 60mA)	100 x 10^{3}	794 x 10^{3}	1 x 10^{15} phs/sec/10%b.w. 1 x 10^{12} phs/sec/0.1%b.w. 1 x 10^{9} phs/pulse/10%b.w. 1 x 10^{6} phs/pulse/0.1%b.w.	5-30 keV
KEK-ERL Low-rep. mode (1nC, 10kHz, 0.01mA)	100 – 1000	10000	1 x 10^{11} phs/sec/10%b.w. 1 x 10^{7} phs/sec/0.1%b.w. 1 x 10^{7} phs/pulse/10%b.w.	5-30 keV
Laser Bunch Slicing (ALS upgrade)	200	40000	5 x 10^{7} phs/sec/0.1%b.w.	0.2-10 keV
Laser-produced plasma X-ray	~100	10	6 x 10^{10} phs/pulse/4πsr	8 keV (Cu-Kα)
Laser / high harmonic generation	100 - 0.1	10 - 10000	~ 10^{8} phs/sec/0.1%b.w.	10 eV-1 keV
Sub-Picosecond Pulse Source (SLAC)	80	10	2 x 10^{7} phs/pulse/1.5%b.w.	8-10 keV
KEK PF-BT line	500	20	~ 10^{7} phs/pulse/10%b.w.	0.2-10 keV
Linac Coherent Light Source (SLAC)	230	120	2 x 10^{12} phs/pulse/0.2%b.w.	1-10 keV

X-ray beam characteristics from superconducting-linac-based Laser-Compton X-ray sources

- **High repetition frequency** (< 1GHz)
- **Hard X-ray available** (~ 10-100 keV)
- **Short pulse duration** (~ 100 fs)
- **Large beam divergence** (~ 10 mrad)
- **Relatively high average photon flux** (~ 10^{10} photons/sec/~10%b.w. @ 10 kHz)

X-ray beam focusing with multilayer K-B mirrors

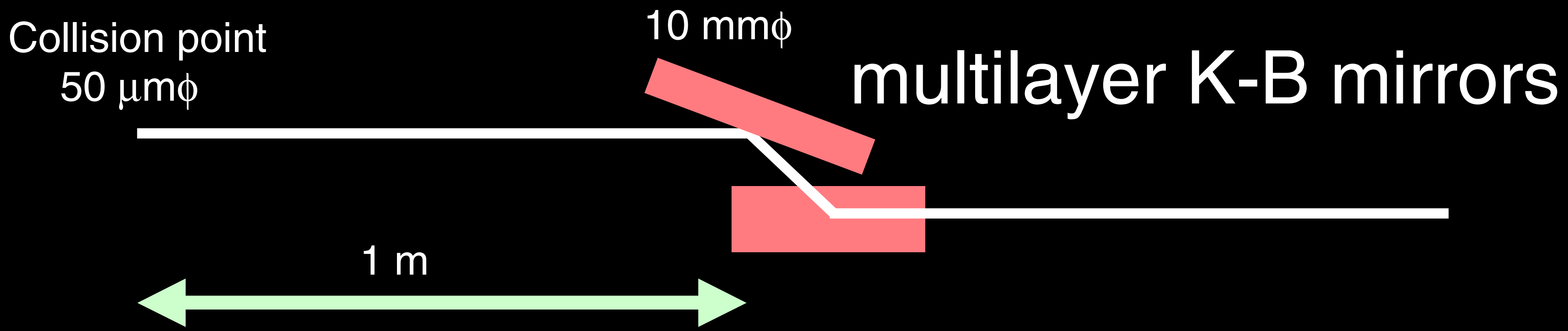

Collision point
50 μmφ

10 mmφ

multilayer K-B mirrors

1 m

Ru/C N80
Size: 300mm(L)
d-spacing: ~20 A
X-ray energy: 30 keV (0.4 A)
Bragg angle: 0.59 degree (10.3 mrad)
Reflectivity: > 80%
deltaE/E: 6-7%

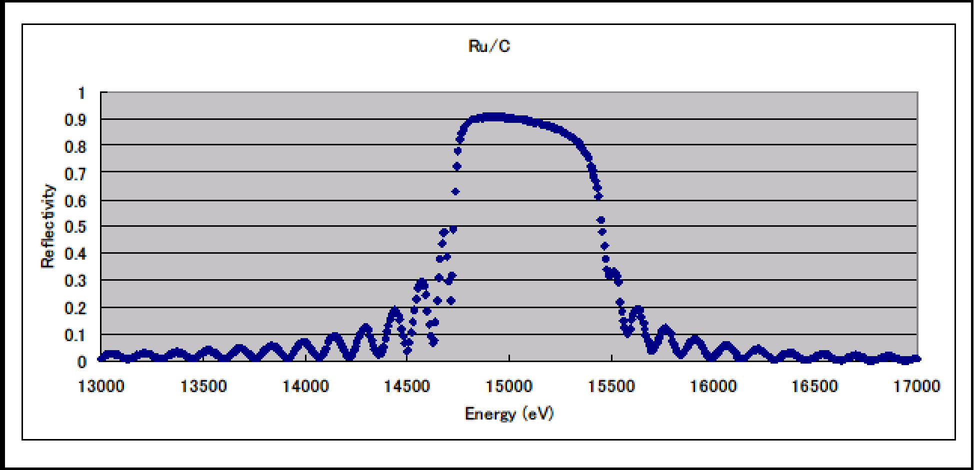

Beam acceptance: 0.3 x 10.3 = 3.1 mm

Other issues to be addressed …

- Timing jitter
- Timing and beam position monitor
- Laser-electron collision
- Bunch compression
- Shot-by-shot fluctuation
- etc…

Motivations for femtosecond X-ray
ex.) reaction dynamics in solution @ NW14

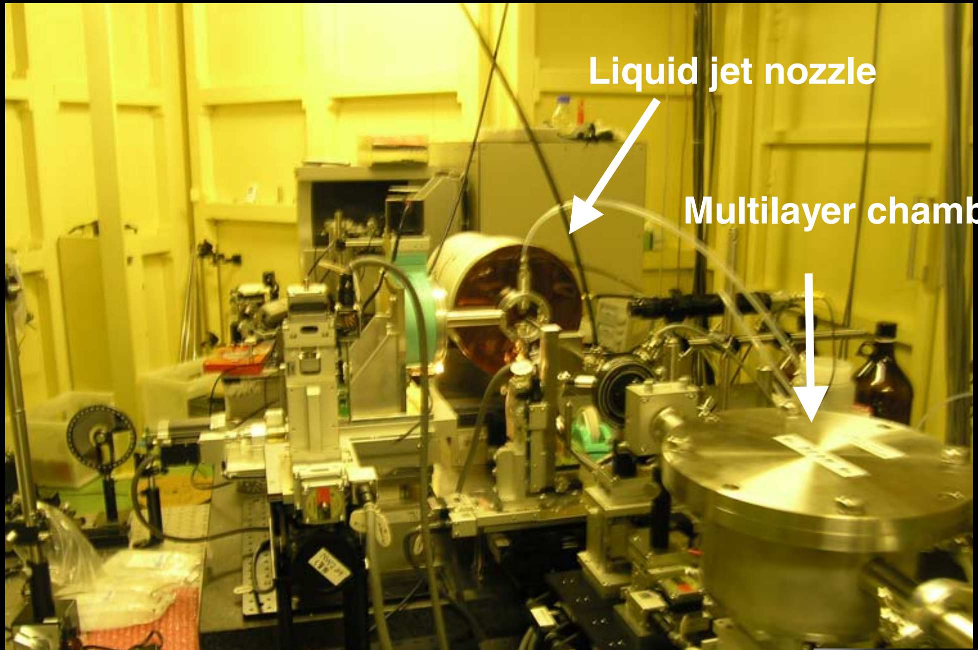

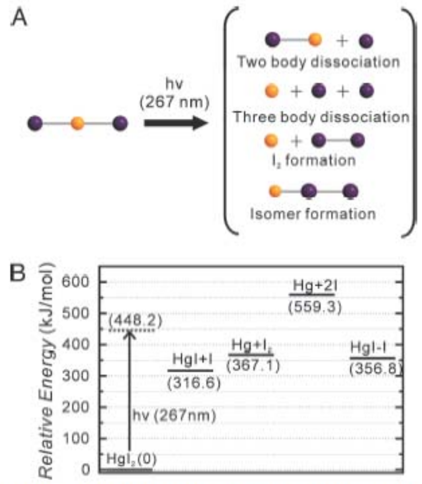

Fig. 1. Schematic diagram for reaction channels and energies in photodissociation of HgI_2 in solution. (*A*) Putative reaction channels after photodissociation of HgI_2 in solution. (*B*) Relative energies of the dissociation products of HgI_2 in solution. All values were calculated by density functional theory.

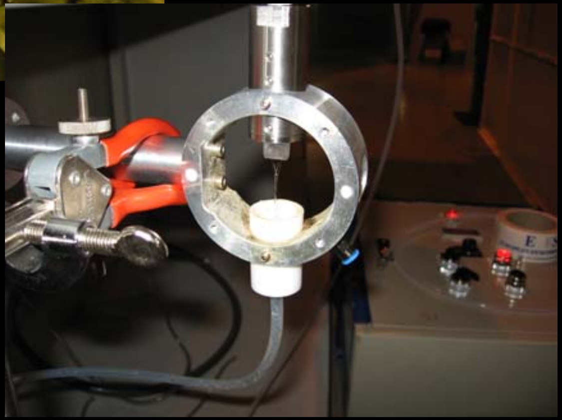

Collaboration with Hyotcherl Ihee Group (KAIST, Korea)

Solution scattering profiles

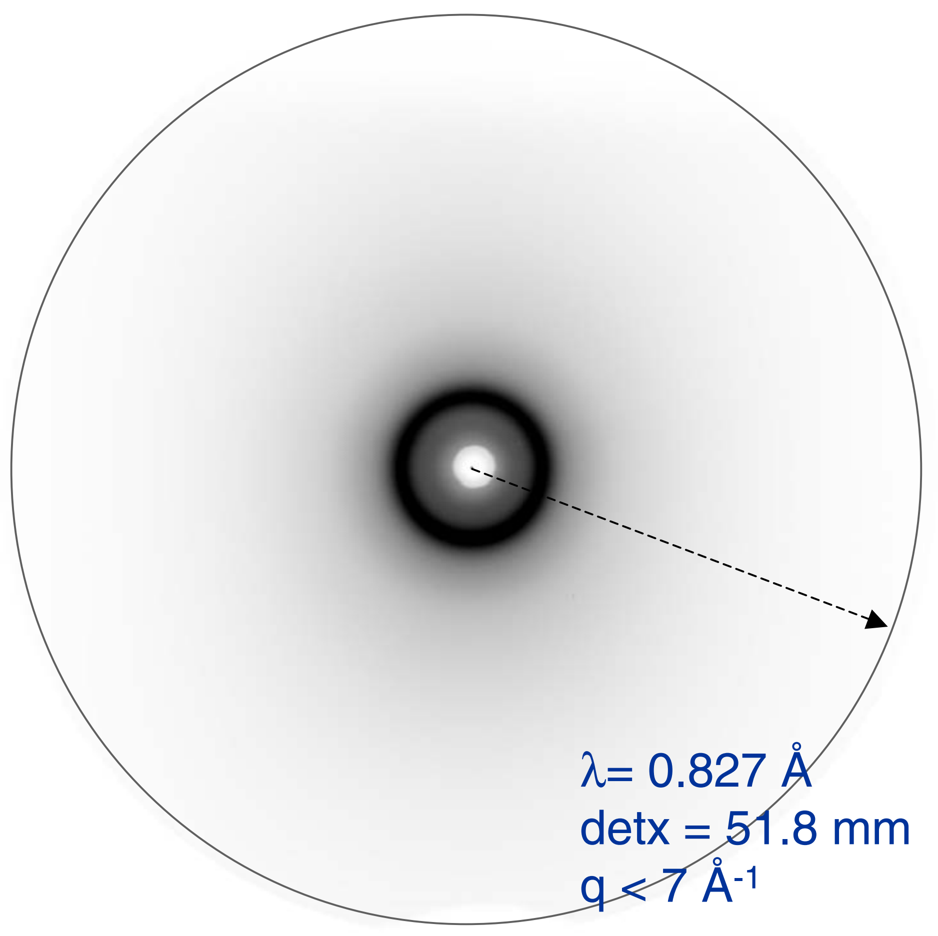

λ= 0.827 Å
detx = 51.8 mm
q < 7 Å^{-1}

- Before Calibration; detx=55

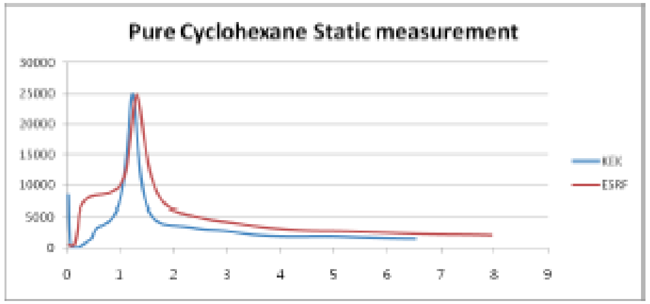

Pure Cyclohexane Static measurement

- After Calibration; new detx=51.8

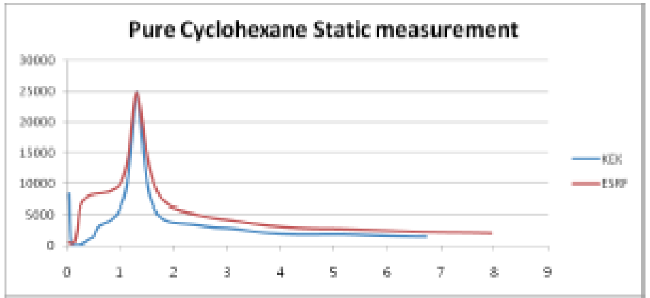

Pure Cyclohexane Static measurement

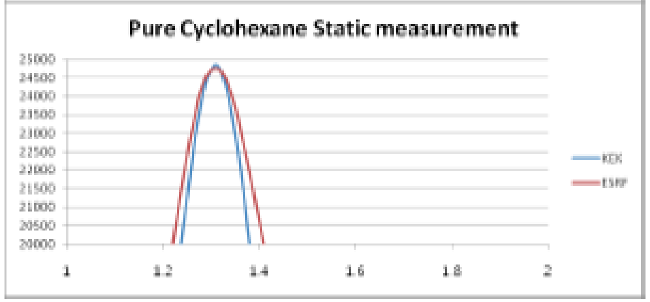

Pure Cyclohexane Static measurement

Photoreaction of I_3^- in methanol

$I_3^- + h\nu \rightleftarrows I_2^{\bullet -} + I^\bullet$

Difference liquid scattering profile

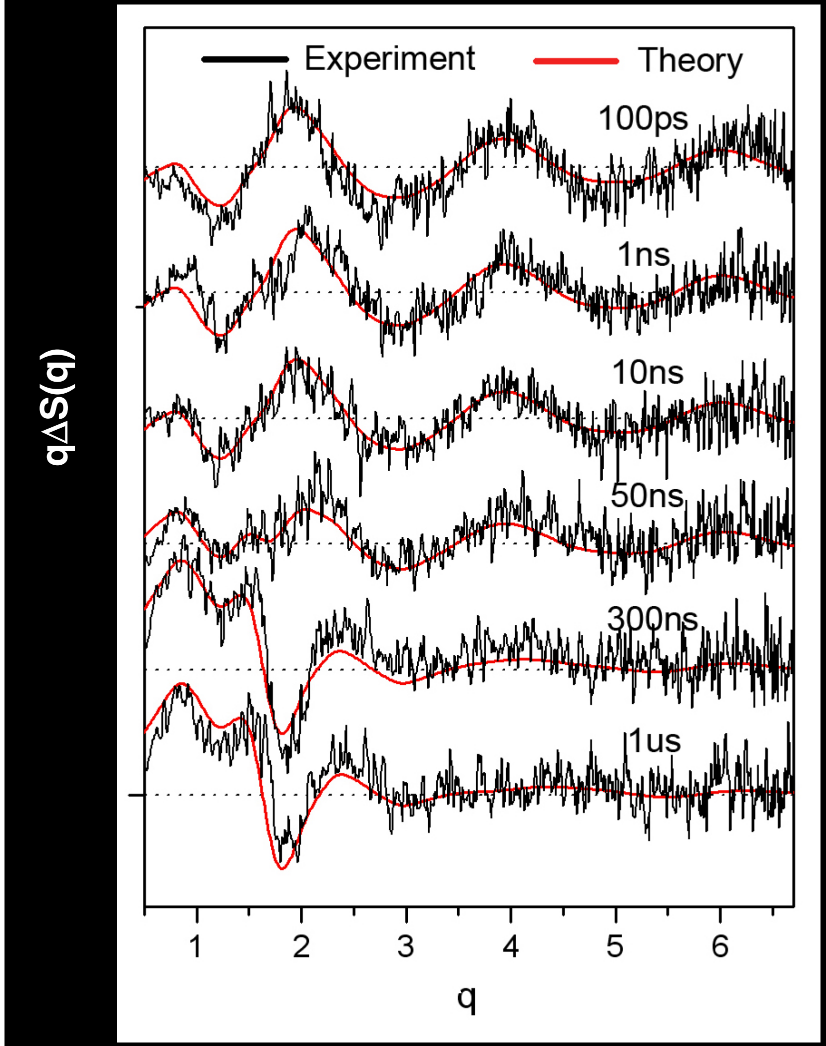

- 50 sec exposure for 1 image
- 10 repetitions for each time delay
- 15 mM I_3^- solution
- Laser: 400 nm, 60 μJ/pulse

Reaction time course

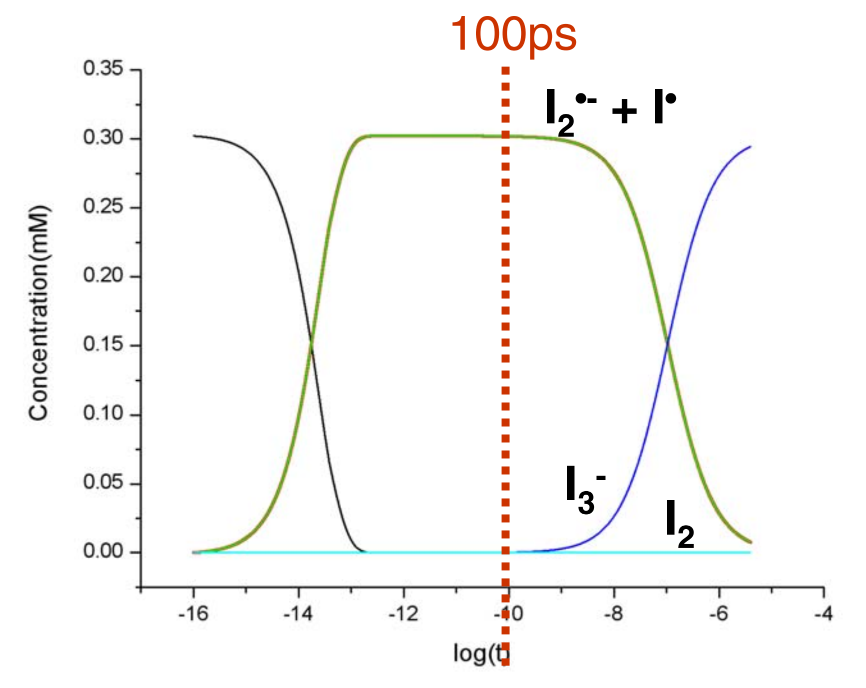

UV spectroscopy revealed dumped oscillations in femtosecond time domain

Caging and Geminate Recombination Following Photolysis of Triiodide in Solution

Gershgoren et al., *J. Phys. Chem. A* **1998,** *102,* 9-16

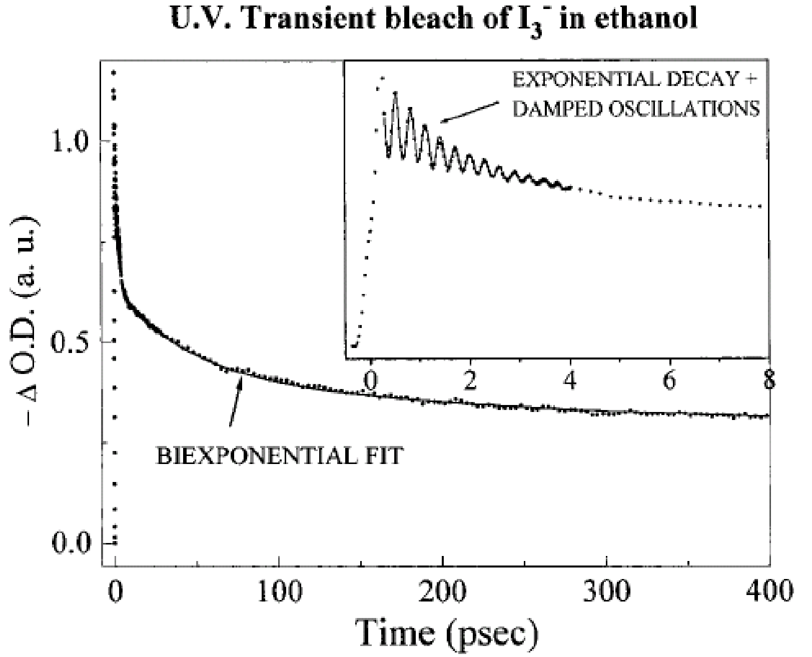

Figure 1. Transient transmission scans of triiodide in ethanol solution with both UV pump and probe pulses. The inset depicts the first 8 ps of probe delays, exhibiting a rapid decay of the initial bleach superimposed by impulsive Raman-induced spectral modulations. See text for details.

Other applications at NW14 which might be suitable for femtosecond X-ray studies

Type of experiments	sample	Typical repetition rate
Single-crystal diffraction	Charge transfer complex crystal	1kHz
	Transition metal oxides	1kHz
	Protein crystal	1 Hz
Liquid scattering	Organic & inorganic solution	1kHz
	Protein solution	1kHz
XAFS	Transition metal complex solution	1kHz

Coherent diffraction imaging?

Direct measurement of antiferromagnetic domain fluctuations

Shpyrko et al. Nature (2007) 447, 68-71.

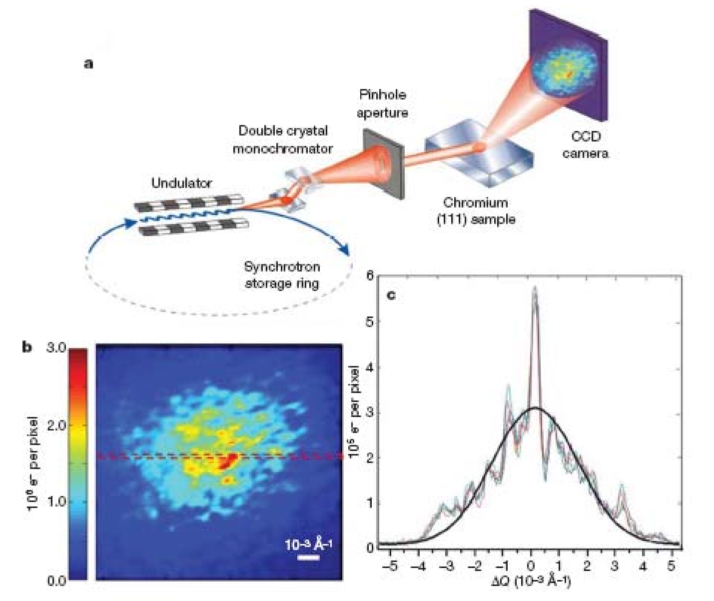

Figure 2 | X-ray speckle measurements. a, Diagram of the experimental set-up. **b**, CCD image of the X-ray speckle observed for the [200] lattice Bragg reflection. **c**, Intensity distribution for a line scan across the region between the dashed lines in **b**. Five differently coloured and nearly identical lines represent line scans of the portion of speckle pattern shown between the red dashed lines in **b**, taken one hour apart. The black line is a simulated statistically averaged gaussian profile, expected for a completely incoherent beam.

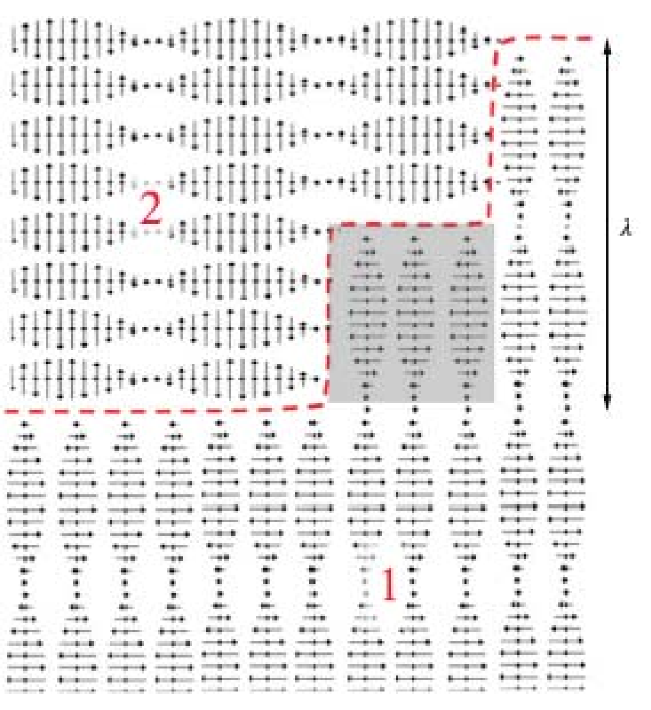

No!

$\lambda = 1$ Å, $\Delta x = 50\ \mu$mのとき、

$\Delta x \bullet \Delta\theta = \lambda / 4\pi \sim 10^{-11}$ mrad

$\Delta\theta \sim 10^{-11} / 50\mathrm{x}10^{-6} = 2 \mathrm{~x~} 10^{-7}$ rad $= 0.2\ \mu$rad

Short pulse + X-ray imaging ?

X-ray Imaging of Shock Waves Generated by High-Pressure Fuel Sprays
MacPhee et al. **Science (2002) 295, 1261.**

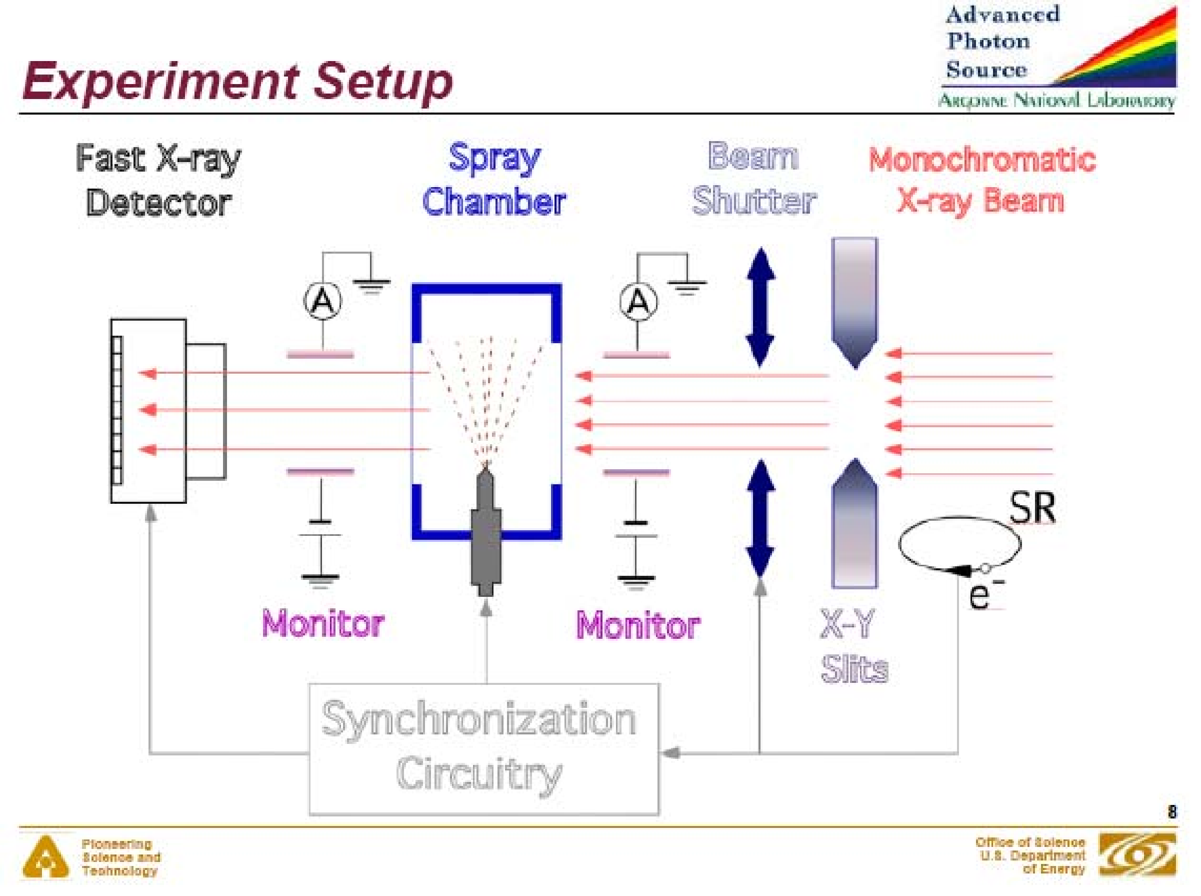

Experiment Setup

Advanced Photon Source
Argonne National Laboratory

8

Pioneering Science and Technology

Office of Science U.S. Department of Energy

see video!

Medical imaging ?

- **Hard X-ray available** (~ 10-100 keV)
- **Large beam divergence** (~ 10 mrad)
- **Relatively high average photon flux** (~ 10^{10} photons/sec/~10%b.w. @ 10 kHz)
- **Relatively compact setup**